Article

LNG Bunkering QRA: A Case Study on the Port of Piraeus

Nikolaos P. Ventikos [1], Vasileios C. Podimatas [1,*] and Alexandros Koimtzoglou [1]

[1] Laboratory for Maritime Transport, School of Naval Architecture & Marine Engineering, National Technical University of Athens, Zografou (157 73), Attika, Greece

[*] Correspondence: vasileiospodimatas@mail.ntua.gr

Abstract: The use of LNG as maritime fuel is a viable option when it comes to reducing the harmful emissions produced by vessels throughout the world, to comply with IMO's Annex VI requirements. However, since the concept is gaining constant focus, special attention must be paid, so that stakeholders fully comprehend LNG's unique properties and hazards, as well as be aware of the standard procedures and best practices that must be followed when handling and storing LNG. In this paper, a Quantitative Risk Assessment (QRA) methodology is presented along with its application on an LNG bunkering case study at the Port of Piraeus. As a result, LNG's properties are considered, potential hazards are identified, failure frequencies are determined, and accidental consequences are modelled. Having evaluated these parameters, Individual Risk (IR) is assessed, safety distances are outlined, risk drivers are identified.

1. Introduction

Regulations regarding the air emissions from ships, are getting stricter every few years. The Heavy Fuel Oil (HFO) that vessels consume, contains roughly 2.7 thousand times more sulphur than the fuel being used for road transportation [1]. Sulphur oxides (SO_X) cause serious environmental issues like soil acidification and harm the biodiversity of the ecosystem. It has also been proven that inhaling sulphur dioxide (SO_2) even for a short 10-minute period, may hurt the respiratory system and lungs [2]. All the above, are advocated by research that identifies the shipping industry's harmful exhaust gas emissions, as a considerable contributor to annual health costs [3].

The International Maritime Organization (IMO) published the first iteration of Annex VI in 2005, where issues that are relevant to restricting the atmospheric pollution caused by ships are addressed. Among the topics that are being dealt with, is the establishment of Emission Control Areas (ECAs), which have stricter emission limits than the rest of the world [4].

The three most common ways of abiding by these regulations, are the use of exhaust gas scrubbers, the consumption of Low-Sulphur Fuel Oil (LSFO) and the use of alternative marine fuels, such as Liquefied Natural Gas (LNG) [5]. LNG carriers have been utilizing LNG as a secondary fuel for over 40 years to exploit the, otherwise wasted, emissions of Boil-Off Gas (BOG). However, the first vessel that relied exclusively on LNG for its propulsion, was M/F GLUTRA [6], a Norwegian car ferry built in 2000. The most significant benefits of using LNG as fuel, are its relatively low price compared to other conventional fuels, in addition to its extremely low sulphur content. LNG

produces about 90% less SO$_X$, nitrogen oxides (NO$_X$) and particulate matter (PM), as well as 30% less carbon dioxide (CO$_2$) [7]. LNG bunkering standard practices can be found in IOGP's (International Association for Oil and Gas Producers) "Guidelines for Systems and Installations for Supply of LNG as Fuel to Ships (ISO 118683, 2015)" [8] as well as DNV's "Development and Operation of Liquefied Natural Gas Bunkering Facilities (2015)" [9].

The main objective of this paper is to present and analyse a QRA methodology that is novel to the LNG bunkering industry. Simultaneously, to validate its effectiveness, it is applied on an LNG bunkering case study at the port of Piraeus. The bunkering concepts modelled are the Truck-To-Ship (TTS) and Ship-To-Ship (STS) operations. A brief comparison of their features is shown in **Table 1**. It is noted that the STS bunkering concept can accommodate larger bunker quantities than TTS.

Table 1. TTS & STS pros & cons.

Bunkering Method	Capacity (m³)	Rate (m³/h)	Pros	Cons
TTS	50-100	40-60	Flexibility, Low capital investment	Limited capacity and rates, Hinders SIMOPS[1]
STS	100-6500	500-1000	Flexibility, High capacity & rates, doesn't hinder SIMOPS	High capital investment

Similar efforts, towards quantifying risk related to LNG bunkering, has been identified in the work of DNV [1], and [10]. However, the work presented in this paper, differs in the aspects of the work presented by the similar studies. For instance, the presented methodology employs a dissimilar consequence model that the respective effort by DNV, and the one by Fluxys LNG, follows different structure for the application of the methodology.

1.1. LNG Properties and Hazards

Natural gas (NG) predominantly consists of methane (70-99% m/m). It also contains traces of other light hydrocarbons such as ethane, propane, and butane [11]. LNG occurs when methane vapor is cooled down to -162 °C at atmospheric pressure and hence, it constitutes a cryogenic liquid. It is beneficial to have it retained in liquid state due to its reduced volume [12]. Its density is about half the density of sea water and thus, when it leaks onto the sea, it floats. Methane vapours that are below -100 °C, are heavier than air and as a result, when an accidental release occurs, at first, LNG vapor will hover over the sea surface, until enough heat is conducted through the air and its temperature becomes higher than -100 °C [13]. After that point, the vapor becomes buoyant and disperses downwind. LNG is also about half as dense as HFO, while its calorific value is approximately 20% higher. As a result, for a ship to attain the same range on LNG, she has to bunker about 1.8 times more fuel [7].

NG is not flammable when liquid. Methane vapours however, are. When the volumetric ratio of methane to air is in the range of 5-15% v/v, the mixture is considered flammable. The 5% concentration is also known as the Low Flammable Limit (LFL), whereas the 15% is the Upper Flammable Limit (UFL) of NG [14]. Methane is colourless. However, when cold LNG vapor escapes in the atmosphere, due to its low temperature, it causes the surrounding air to condensate, thus, creating a characteristic white cloud over the surface of the substrate [15]. LNG is considered a low-

---

[1] Simultaneous Operations

flashpoint fuel [16]. The thermal hazards posed by an accidental release of LNG are [11]: thermal radiation due to fire, local overpressure build-up due to Vapor Cloud Explosion (VCE) and/or Rapid Phase Transition (RPT), freeze burns and asphyxiation. The predominant hazard posed by an LNG release is thermal radiation emitted by fire. According to the Institute of Chemical Engineers (IChemE), in the instance of an LNG pressurized release where ignition occurs, the potential consequences are Fireball/BLEVE (Boiling Liquid Expanding Vapor Explosion), VCE, Jet Fire, Flash Fire and Pool Fire [17].

A summary of the rest of the paper is as follows. In Section 2, the proposed quantitative risk assessment framework is laid out. In Section 3, an application of the risk model is presented with a case study at the port of Piraeus. In Section 4, a brief discussion concerning the points of consideration and challenges that a QRA entails is provided, while the results of Piraeus' case study are compared to outcomes from similar studies conducted by DNV and Fluxys. Finally, in Section 5, the main conclusions of this study are outlined.

2. Methodology

Risk assessment is a technique that has been utilized by humanity throughout most of its recorded history [18]. In its simplest form, a risk assessment consists of a model that analyses probability and consequence and assigns them non-numerical (qualitative) values. While simple in concept, a qualitative risk assessment (QualRA) has proven useful many times for decision makers [19]. However, it presents a multitude of limitations when it comes to modelling complex systems that require the incorporation of time-reliant events which entail several actions with multiple outcomes. Hence, on many occasions a more potent risk assessment tool is required, i.e., a QRA.

A QRA is a much more elaborate process than a QualRA [20]. Since failure frequencies and potential consequences in the event of an accidental event must be quantified, extensive system knowledge, is a prerequisite for performing a QRA. In general, every QRA commences with a HazID process where the goal is to identify a set of credible hazards that can lead to system failure. Through the HazID, several plausible failure scenarios may be assumed, which is a process commonly referred to as failure case estimation. Every scenario of the failure case estimation is analysed extensively, to determine its failure frequency, as well as model the potential consequences that may occur from its fulfilment. The result of the above procedure is the quantification of risk, which is then compared to a set of well-established set of risk criteria, to complete the system's risk assessment. The outcome of a QRA is commonly the Individual Risk or Societal Risk of the system. A generic QRA process in block diagram form, is shown in **Figure 1**.

Individual Risk (IR) is defined as the probability of an individual's death due to an accidental event in an establishment, within the duration of a year (12 months). It is graphically portrayed as IR iso-contours, that outline the establishment's areas where risk level is unacceptable, acceptable or negligible and is approximated as [22]:

$$IR = \sum_S \sum_M \sum_\varphi \sum_i \Delta IR_{S,M,\varphi,i}$$

Where $\Delta IR_{S,M,\varphi,i}$ is the contribution of the loss of containment event S, the weather class M, the wind direction φ, and the ignition event i, to the total IR at a given grid point. All the parameters mentioned above will be analysed in the following sections.
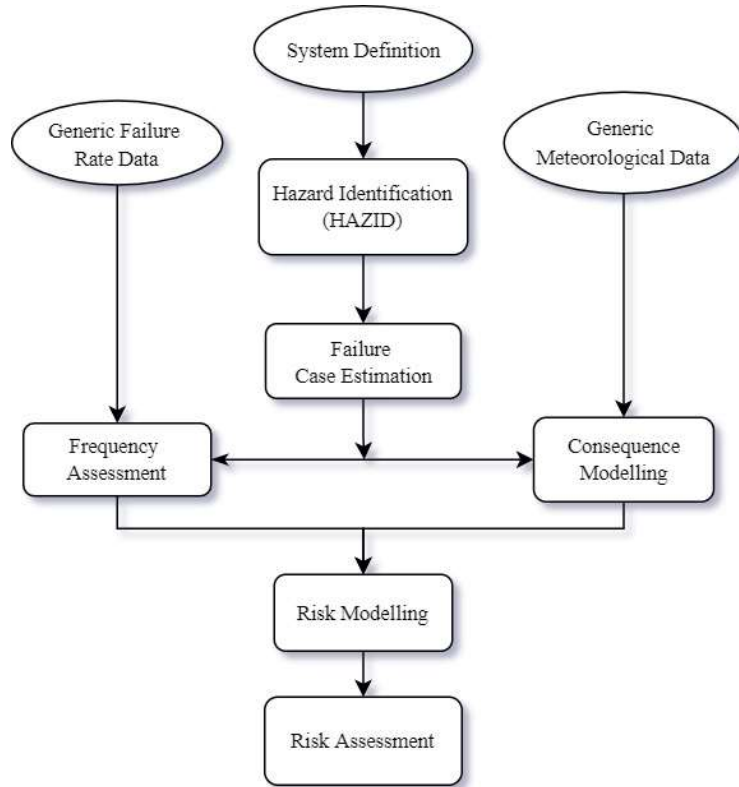
Figure 1. Typical Quantitative Risk Assessment [21].

2.1. Selection of Installations

QRAs are utilized in safety analyses to demonstrate the risk caused by an establishment, and to further assist the decision-making process of a regulatory body. An establishment consists of a variety of installations, e.g., a port may have quays, jetties, platforms, storage areas, offices, etc. However, not all the installations contribute significantly to the total risk of the establishment and as a result, it is not worthwhile to include all of them in the QRA process. The selection method followed in this study, is presented in **Figure 2**.
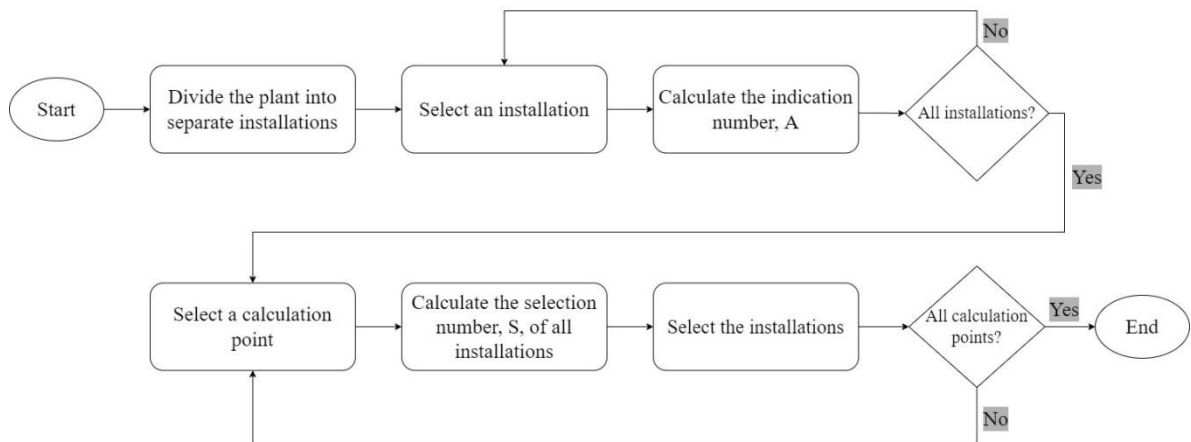

Figure 2. Installation selection procedure [22].

Initially the establishment is divided into several separate installations. Two installations, i.e., No.1 and No.2, are considered "separate", if a dangerous substance release from No.1, does not lead

to a significant release in No.2. For instance, process installations are separate from storage installations. Afterwards, the indication number **A** is calculated for every installation. The indication number is a measure of the installation's intrinsic hazard and is defined as:

$$A = \frac{Q_i O_1 O_2 O_3}{G_i}$$

Where: Q_i is the quantity of the dangerous substance i (e.g., LNG) within the installation in kilograms (kg). O_1 is a factor that accounts for the installation type i.e., process or storage, according to Table 2.

Table 2. Factor O_1.

Type	O_1
Process Installation	1.0
Storage Installation	0.1

O_2 is a factor that accounts for the positioning of the installation (i.e., enclosed, bund or outdoors), and accounts for the provisions in place that will hinder the substance's dissemination in the environment, according to Table 3.

Table 3. Factor O_2.

Positioning	O_2
Outdoor Installation	1.0
Enclosed Installation	0.1
Installation situated in a bund, and a process temperature less than the atmospheric boiling point plus 5°C	0.1
Installation situated in a bund, and a process temperature more than the atmospheric boiling point plus 5°C	1.0

O_3 is a factor that accounts for process conditions, and it constitutes a measure of the amount of substance in the gas phase after its release, according to **Table 4**.

Table 4. Factor O_3.

Phase	O_3
Substance in gas phase	10
Substance in liquid phase	10
Substance in solid phase	0.1

G_i is the limit value for explosive substances that is equal to the amount of substance (in kg) which releases an amount of energy equivalent to 1000 kg of TNT (i.e., explosion energy of 4600kJ/kg).

Next, the selection number N is calculated as:

$$N = \left(\frac{100}{L}\right)^3 A$$

Where A is the indication number, and L is the distance from the installation to the specific location, with a minimum of 100m. The selection number is calculated for every installation at a minimum of

8 locations that are on the boundary of the establishment while the distance between two adjacent locations must not be more than 50m.

Finally, according to RIVM [22], for an installation to be selected for a QRA analysis, its selection number must be greater than one (N>1) at a location on the boundary of the establishment and larger than 50% of the maximum selection number at that location.

2.2. Failure Case Estimation

The failure case estimation entails the selection of credible Loss of Containment (LOC) events, henceforth noted as S. A release of a stored hazardous substance, is commonly modelled as either a continuous or an instantaneous release, with each instance having dissimilar properties. In the occasion of LNG bunkering however, such a categorization is unfitting, since it entails the use of hoses and manifolds with pressurized LNG, whereas during a release from a tank, the stored LNG will probably be in atmospheric pressure. As a result, the release is modelled as either a leak or a rupture. A leak is considered to occur when a hose's damaged area is approximately 10% of its total diameter. A rupture is when a full-bore release takes place, meaning that LNG is released through the hose's full diameter e.g., a severed hose.
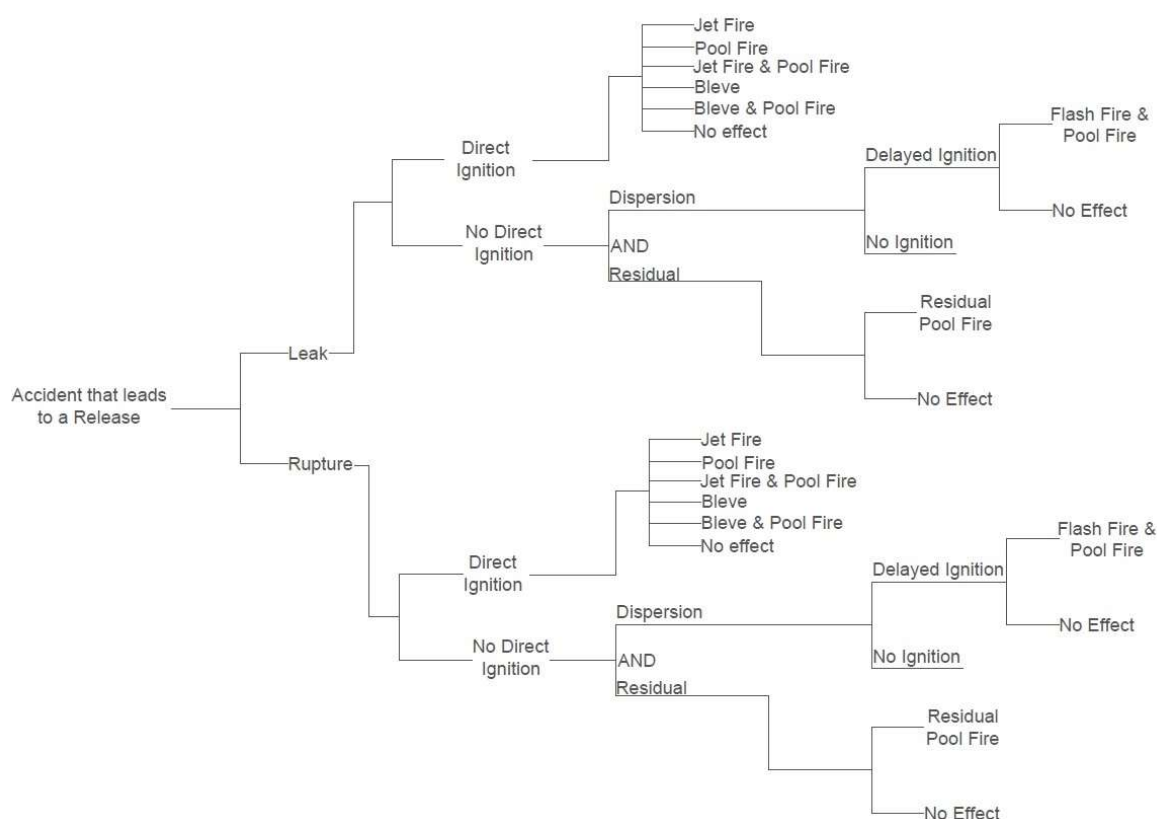
2.3. Failure Frequencies

Figure 3. Event tree of an accidental release during LNG Bunkering.

The failure frequencies, henceforth noted as f_s, for each release scenario are assumed, so that the most recurrent events will become more prevalent compared to the ones that are unlikely to occur. For instance, an LNG hose leak is modelled, assuming that the only two possible adverse outcomes in case of an immediate ignition upon release, is a jet fire and a BLEVE. The thermal radiation that

would be emitted in the instance of a BLEVE, is approximately ten times higher than a jet fire. That would ultimately result in proposed safety distances that are proportionate to the BLEVE's consequences. A BLEVE occurrence however, especially when an LNG related accident is modelled, is an extremely unlikely event. Therefore, by considering the worst-case scenario without considering the frequency of its occurrence, overestimated safety zones are produced. In Figure 3, the event tree of an LNG release during bunkering operations is presented. It is noted that direct ignition has the potential to lead in more catastrophic consequences compared to delayed ignition.

2.4. Consequence Modelling

An atmospheric tank breach will initiate a discharge that predominantly consists of LNG. However, a potential rupture of an LNG bunkering hose or manifold, will result in a pressurized release. LNG will flash out of the damaged area, resulting in a two-phase discharge. The potential consequences in either case is a jet fire, a pool fire, a flash fire, a VCE and/or a fireball/BLEVE (Figure 4).
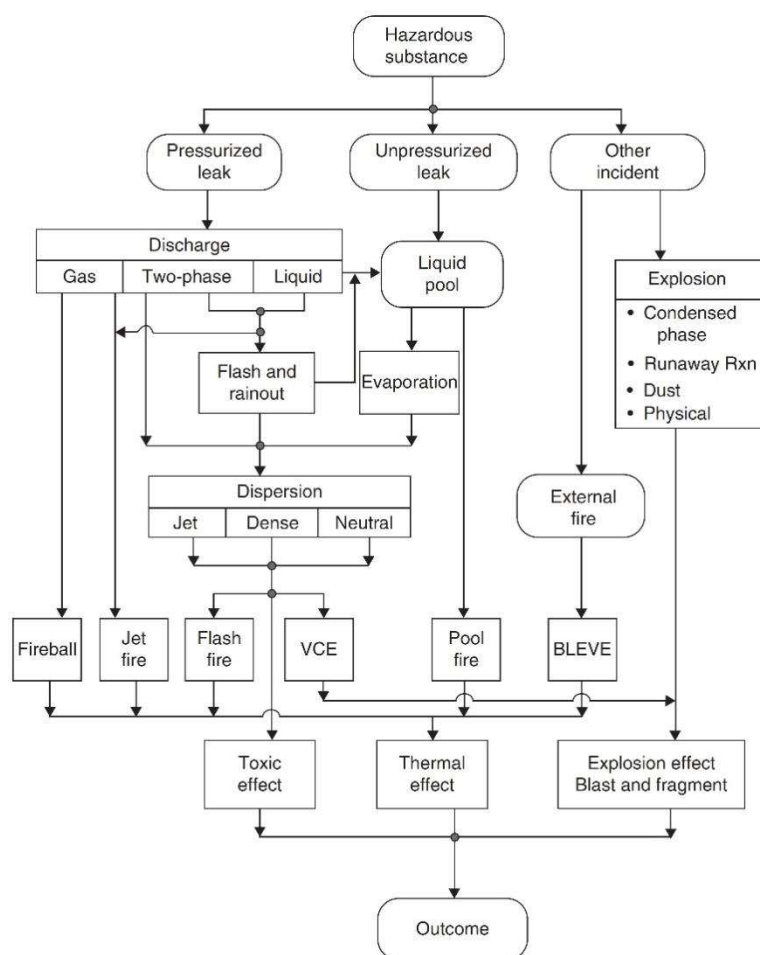

Figure 4. Potential consequences from a release of a hazardous substance [23].

2.4.1. Source Term and Dispersion

The discharge rate of the released LNG is approximated by the Bernoulli equation for sub-cooled liquids [11]:

$$G = \sqrt{2\rho_L \left(P_0 - P_{back} \right)}$$

Where G is the mass flux in $kgm^{-2}s^{-1}$, ρ_L is the LNG's density in kgm^{-3}, P_{back} is the back pressure in Pa, and P_0 is the liquid pressure in Pa.

The discharge rate of a two-phase release, is approximated by the Homogeneous Non-equilibrium Model [24] as:

$$G = \frac{L_C}{\left(v_g - v_l \right)} \sqrt{N c_p T}$$

Where L_c is the specific latent heat of vaporisation in Jkg^{-1}, v_g is the specific volume of the vapour in m^3kg^{-1}, v_l is the specific volume of the liquid in m^3kg^{-1}, c_p is the heat capacity of the fluid in $Jkg^{-1}K^{-1}$, T is the temperature in K, N is calculated as:

$$N = \frac{L_C^2 v_L}{2 \left(P_0 - P_{back} \right) c^2 \left(v_g - v_l \right)^2 T c_p} + \frac{l}{l_e}$$

c is the discharge coefficient, l is the length of the pipe in m, and le is equal to 0.1m. The dispersion characteristics of the natural gas cloud in case of an accidental release, are approximated with the use of an Integral or Heavy Gas Dispersion Model [25].

2.4.2. Ignition

The probability of ignition, henceforth P_i, is a key parameter in many QRAs [26]. Common ignition sources include industrial ovens, boilers, high voltage cables, motor vehicles, houses, ships etc. Upon immediate ignition of the released LNG at the source, a jet fire, a pool fire and/or a fireball will commence. This is referred to as direct ignition. If there is no direct ignition source, the NG's cloud will disperse downwind. At some point, when within the cloud's flammable extent, another ignition source might be present, causing a delayed ignition, that may lead to a flash fire, a VCE, or even a pool fire.

The probability of ignition relies on the cloud's flammable extent and the strength of the ignition source. However, detecting the ignition source, is not always feasible. Historically, there have been many times that even though not a single ignition source could be determined, a fire started anyway [11]. In these instances, ignition was attributed to static electricity charges that originated from poorly grounded equipment.

An approximation of the probability of ignition within an installation, is provided by the following time-dependent formula [26]:

$$P(t) = P_{present} \left(1 - e^{\omega t} \right)$$

Where P(t) is the probability of ignition during the time interval of 0 to t, $P_{present}$ is the probability of the ignition source being present within the cloud's flammable extent, ω is the effectiveness of the ignition measured in s^{-1}, and t is time measured in seconds (s). Empirical values regarding the probability of ignition according to RIVM are presented in **Table 5**. It is noted that a leak is more probable to result in a delayed ignition, whereas a rupture yields higher probability for a direct ignition.

Table 5. Typical values of probability of ignition [26].

	Probability of Ignition, P_i	
LOC Scenario	*Direct Ignition*	*Delayed Ignition*
Leak	0.2	0.25
Rupture	0.5	0.35

2.4.3. Meteorological Data

Meteorological data regarding the establishment of interest are detrimental to the accuracy of the QRA model, since weather has a big impact on cloud dispersion. The information provided by weather stations usually includes wind speed, air temperature, relative humidity, atmospheric stability class and wind direction. The combination of wind speed and atmospheric stability class, is called weather class and is henceforth noted as M, whereas the wind direction is henceforth noted as φ.

Atmospheric stability is a measure of the atmosphere's turbulence. It relies on solar insolation as well as wind speed. The correlation between atmospheric stability, solar insolation and wind speed is shown in **Table 6**. Pasquill [27] and Gifford [28] defined several different stability classes that ranged from A to F. The neutral atmosphere is of class D, which corresponds to a lapse rate of α=0.98°C per 100m of elevation. Therefore:

$$\frac{\partial T_{air}}{\partial z} < \alpha: Unstable, \quad \frac{\partial T_{air}}{\partial z} = \alpha: Neutral, \quad \frac{\partial T_{air}}{\partial z} > \alpha: Stable$$

An unstable atmosphere means that as the altitude increases, temperature rises way too fast. Unstable atmospheric conditions are usually found during the daytime and correspond to classes A, B, C. A stable atmosphere is the opposite; as the altitude rises, the temperature drops rapidly, which is called inversion. Stable atmospheric conditions correspond to classes E and F. Atmospheric stability greatly impacts the cloud dispersion. An unstable atmosphere will cause the cloud to disperse and thin-out faster than a neutral atmosphere.

Table 6. Atmospheric stability classes depending on wind speed and solar insolation [11].

Surface Wind Speed (ms^{-1})	Day			Night	
	Strong	*Moderate*	*Slight*	*Thinly overcast*	*Cloud*
≤2	A	A-B	B	-	-
2-3	A-B	B	C	E	F
3-5	B	B-C	C	D	E
5-6	C	C-D	D	D	D
≥6	C	D	D	D	D

2.4.4. Thermal Radiation

A jet fire occurs when natural gas is immediately ignited upon its release. Jet fires act like a blowtorch and can impinge buildings and process equipment. The main concern, however, is the emitted thermal radiation. For natural gas jet fires, the flame temperature inside the fire can reach up to 1252°C that corresponds to an equivalent blackbody emissive power of 307kWm^{-2} [11]. However,

the reach of a jet fire is very limited. As a result, thermal radiation does not spread over a vast area. The flame's emissive power E in kWm^{-2}, is approximated as [29]:

$$E = \frac{f_{rad} Q \Delta h_c}{A}$$

Where Q is the discharge rate in kgs^{-1}, Δh_c is the heat of combustion in Jkg^{-1} and A is the flame's surface area in m^2. The fraction of heat the flame's surface irradiates is approximated as:

$$f_{rad} = 0.12 C_{MW} exp\left(-0.00323 u_j\right) + 0.11$$

Where C_{MW} is a correction factor that depends on the molecular weight of the substance. The gas velocity in the expanding jet is:

$$u_j = M_j \sqrt{\frac{\gamma_g R_c T_j}{W_{gk}}}$$

Where T_j is approximated as:

$$T_j = \frac{2T_s}{2 + (\gamma - 1) M_j^2}$$

M_j is the Mach number of the expanded flow, that for an unchoked flow is given by:

$$M_j = \left[\frac{\left(1 + 2\left(\gamma_g - 1\right) F^2\right)^{1/2} - 1}{\left(\gamma_g - 1\right)}\right]^{1/2}$$

$$F = 3.6233 \cdot 10^{-5} \frac{Q}{d_0^2} \sqrt{\frac{T_S}{\gamma_g W_{gk}}}$$

Where d_0 is the diameter of the orifice in m, Q is the mass release rate in kgs^{-1}, γ_g is the ratio of specific heats, W_{gk} is the substance's molecular weight in $kgmol^{-1}$, and R_c is the gas constant equal to $8.3144 JK^{-1}mol^{-1}$.

A pool fire is usually started either via a jet fire or a flash fire. A pressurised discharge results in a two-phase release. Therefore, both NG and LNG, commonly referred to as rain-out, will escape containment. If the gas is directly ignited upon its release, a jet fire will be formed. If the rupture's release rate is high enough as well, a liquid pool will be formed. In that instance, fire will spread from the jet to the evaporating LNG pool, thus starting a pool fire. In the scenario where no direct ignition occurs, an LNG pool as well as a flammable vapour cloud will form. Upon delayed ignition of the cloud, a flash fire will commence. Flash fires attain high temperatures but for very short periods of time and have the tendency to "flash" back to the evaporating pool. Hence, a pool fire is started once again. The average emissive power E of a pool fire in kWh^{-1}, can be approximated as [30]:

$$E = \frac{f_{rad} \Delta h_c \dot{m}}{1 + 4\frac{h}{d}}$$

Where h is the flame length in m, d is the diameter of the pool in m, Δh_c is the heat of combustion in Jkg^{-1}, f_{rad} is the fraction of energy that is released as thermal radiation, and $\dot{m}$ is the areal mass burn rate in $kgm^{-2}s^{-1}$ calculated as:

$$\dot{m} = 0.001 \frac{\Delta h_c}{\Delta h_v + c_p \left(T_b - T \right)}$$

Where c_P is the specific heat capacity in $Jkg^{-1}K^{-1}$, T_b is the ambient boiling temperature in K, Δh_v is the vaporisation heat in Jkg^{-1}, and T is the pool temperature in K.

A flash fire occurs when a flammable cloud ignites. A fast, practical way to determine whether the NG cloud is within the flammable range, is via the plume's visibility. A visible cloud means that NG is in its dense gas phase, hence, the cloud is flammable [7]. Once combusted, flash fires have the tendency to expand in space. If the flame front reaches an area of the cloud where the NG to air mixture is rich, the flame will rise, forcing any unburned fuel up as well.

Atmospheric turbulence is also a prominent contributor as far as flash fires are concerned [13]. Flammable clouds have variable form and concentration along their extent, depending on release conditions, wind speed, ground roughness and atmospheric stability. Consequently, due to local "pockets" of gas, there might be considerable uncertainties when estimating a cloud's maximum LFL extent. To account for that, instead of considering only the LFL area, the 0.5 LFL extent is also entailed in the analysis. Hence, the flammable pockets are being considered, by enlarging the area over which a flash fire could commence.

There are very few studies that provide information on the effects of thermal radiation emitted by a flash fire. Probably because in the event of a flash fire, even in a space that is partially confined, the main concern will be the blast radius due to the explosion, and not the emitted thermal radiation. In this paper, it is assumed that the threat zone of a flash fire is proportionate to the maximum extent of 0.5 LFL area.

For a VCE to have catastrophic repercussions over an installation, 3 conditions have to pre-exist [11]: a highly reactive fuel, a strong ignition source and a confined space. Even though a strong ignition source is always a possibility, methane and LNG mixtures are of low reactivity and hence do not detonate. Furthermore, loading docks typically do not include enclosed or confined spaces.

A fireball is an accidental phenomenon that has the potential to induce thermal radiation hazard distances that are greater than those of a pool fire. There are two types of fireballs, depending on the way they are formed: fireballs that occur from a pressurised release due to a BLEVE and fireballs that occur from the ignition of a large volume of flammable vapours at atmospheric pressure.

A BLEVE is an accidental event capable of generating high energy explosions of tanks containing gas or highly pressurised liquids, leading to successive explosions and fires to other surrounding equipment [31]. It is not a common occurrence in the LNG industry. In fact, three studies that were conducted in 2004 by DNV, Sandia Laboratories and ABS, on marine transport hazards, identified a BLEVE as an either impossible or improbable hazard when it comes to LNG [11]. LNG is predominantly stored and transported at atmospheric pressures. Therefore, if the PRV[2] is correctly adjusted and operates properly, the interior pressure will be ambient, and the tank will remain intact. Even if the tank gets impinged and ruptures, LNG will not violently flash out and thus, a potential

---

[2] Pressure Relief Valve

BLEVE is averted. Nevertheless, according to ISO 20519 [32], when conducting a QRA on an LNG bunkering installation, a BLEVE modelling has to be included. The emissive energy flux of a fireball in case of a BLEVE is approximated in kWm² as [33]:

$$E = 350,000\left(\frac{\Delta h_c}{\Delta h_{c,\,propane}}\right)$$

where Δh_c is the heat of combustion of NG in Jkg⁻¹, and $\Delta h_{c,\,propane}$ is the heat of combustion of propane in Jkg⁻¹. According to AIChE [34], a reasonable emissive energy flux for large hydrocarbon fireballs is 350,000 kWm².

2.4.5. Exposure

The probability of death, henceforth P_D, due to thermal radiation is approximated by the following formula [35]:

$$P_D = 0.5\left[1 + erf\left(\frac{Pr - 5}{\sqrt{2}}\right)\right]$$

Where erf is an error function, and Pr is the probit function for lethality approximated as:

$$Pr = -36.38 + 2.56\ln\left(tq^{3/4}\right)$$

t is the exposure duration in s, q is the thermal radiation in Wm⁻².

2.5. Grid Definition

The purpose of this step is to define a grid of cells that span over the installation of interest. The geometric centre of each cell is called the grid point and the IR is calculated separately for every grid point. Selecting the appropriate grid cell size is of paramount importance. The goal here, is to select as large cells as possible whilst the calculated IR does not significantly vary much within the same cell.

2.6. Individual Risk Calculation

The IR contribution $\Delta IR_{S,M,\varphi,i}$ of the LOC event S, the weather class M, the wind direction φ, and the ignition event i, to the total IR at a given grid point, is measure in y⁻¹ and calculated as [22]:

$$\Delta IR_{S,M,\varphi,i} = f_s P_M P_\varphi P_i P_d$$

Where fs is the failure frequency of a LOC event, P_M is the weather class probability, P_φ is the probability of wind direction, P_i is the probability of ignition, and P_d is the probability of death. In Section 3, the probabilities mentioned above, are presented in greater detail.

After each calculation step is repeated for every ignition event, all weather classes and wind directions, and every LOC scenario, the total Individual Risk at the selected grid point is approximated as:

$$IR = \sum_S \sum_M \sum_\varphi \sum_i \Delta IR_{S,M,\varphi,i}$$

Following the same procedure for every single grid point, the total IR distribution over the area of the installation, can be calculated.

3. Case Study on the Port of Piraeus

In this section, the case study at the port of Piraeus is presented. The QRA model that is outlined in Chapter 2 will be utilised.

The establishment of interest is the port of Piraeus, Greece. Following the procedure described in section 2.1, the selected installations are the quay through which several ferries serve the Piraeus-Crete route (**Figure 5**) as well as the Piraeus' container pier, where container-ships dock to load/unload their cargo (**Figure 6**). The white dot with the crosshair in either site, represents the source of the release.

Figure 5. RoRo quay at the port of Piraeus.

The Loss of Containment events (S) utilised, are summarised in **Table 7**. It should be noted that tank rupture from ship striking is a credible accident scenario only during STS operations. Rupture diameters that are greater than 250mm are not considered since it was deemed superfluous. Besides being built to withstand external impacts, LNG bunker tanks, are very well protected through their placement within the vessel's structure. Therefore, for an accident to cause the catastrophic failure of such a tank, it would also signify the demise of the vessel's hull [11], which is a far more serious predicament, and it is outside of this study's scope.
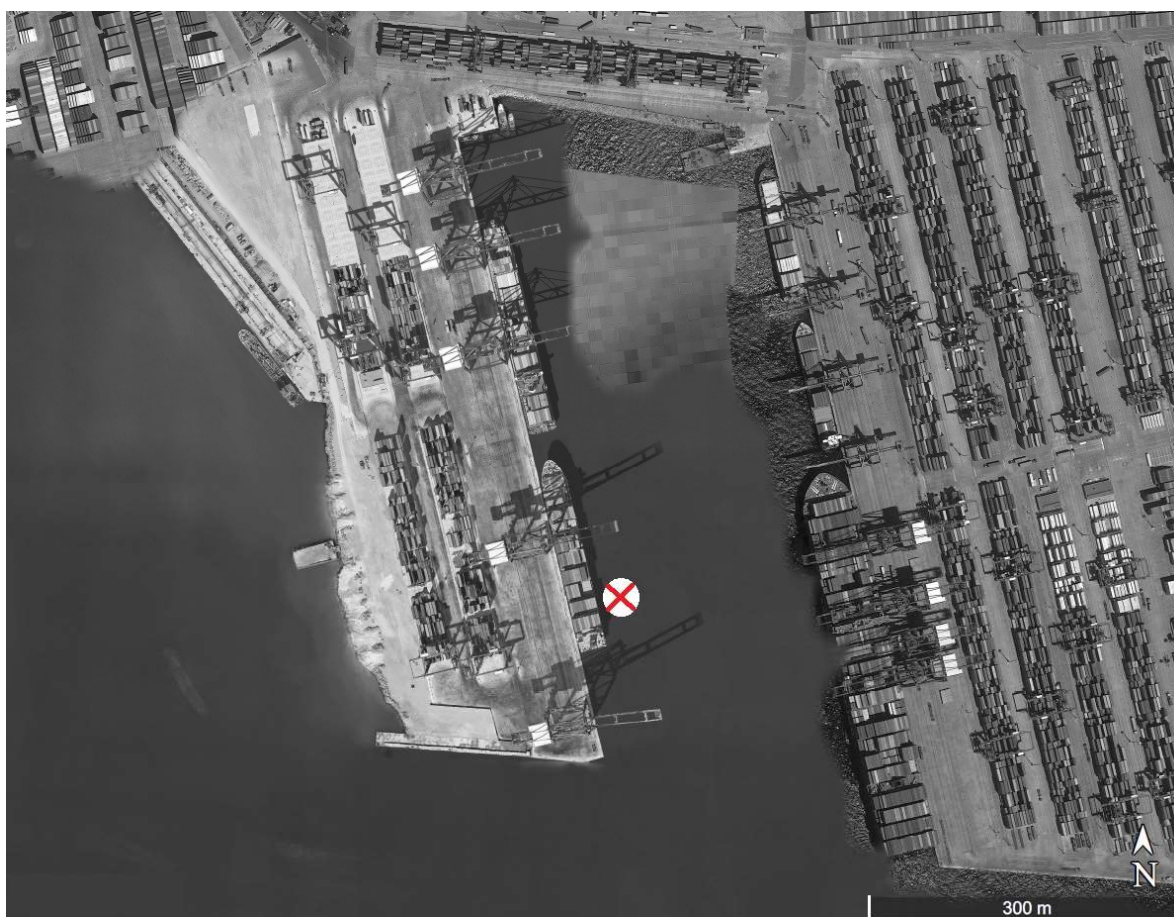
Figure 6. Containership pier at the port of Piraeus.

Table 7. Representative Loss of Containment Scenarios.

Scenario	Equivalent Diameter (mm)
Hose Leak	10% of Hose's Diameter
Hose Rupture	Full Bore
Manifold Leak	10% of Manifold's Diameter
Manifold Rupture	Full Bore
Tank Rupture from S.S.[3]	250
Hose Rupture from S.S.	Full Bore

The failure frequencies (f$_S$) used, sorted by the type of LOC, are shown in **Table 8**. It is noted that the hoses' failure frequency is per hours of operation, whereas the manifolds', is per meters of total length. The ignition probabilities that were utilised are shown in **Table 5**.

In **Table 9**, **P$_M$** is the weather class probability column, which corresponds to a certain atmospheric stability class and wind speed (e.g., D 1.5 ms^{-1}). Consequently, the probability of Piraeus having an atmospheric stability of class D with a wind speed of 1.5 ms^{-1}, is *0.89*. **P$_φ$** is the wind direction probability row, where the corresponding direction that the wind is coming from is shown. Therefore, the probability of a wind that stems from NWW is *0.23*. All the other cells in between, stem from the product of **P$_M$· P$_φ$**, which is required to determine the contribution of each weather class, wind direction and wind speed combination, to the total individual risk. It is noted that the most

---

[3] Ship Striking

probable weather scenario is the {D, 1.5 ms^{-1}, NWW} with a probability of 0.23·0.89=0.205. The following table occurred after statistical analysis of data provided by the Piraeus weather station [36].

Table 8. LOCs and respective failure frequencies [22].

Scenario	Failure Frequency (y^{-1})		
	TTS	*STS*	*STS*
	RoRo	*RoRo*	*Cont/ship*
Hose Leak	1.5·10^{-4}/h	7.3·10^{-5}/h	6.2·10^{-5}/h
Hose Rupture	1.5·10^{-5}/h	7.3·10^{-6}/h	6.2·10^{-5}/h
Manifold Leak	1·10^{-5}/m	5·10^{-6}/m	5·10^{-7}/h
Manifold Rupture	2·10^{-6}/m	1·10^{-6}/m	1·10^{-7}/m
Tank Rupture from S.S.[4]	N/A	1.25·10^{-8}/h	1.25·10^{-8}/m
Hose Rupture from S.S.	N/A	0.006·f$_0$[5]	0.006·f$_0$

Table 9. Weather table for Piraeus.

	Piraeus P$_M$·P$_\varphi$								
	N-NE	*NE-E*	*E-SE*	*SE-S*	*S-SW*	*SW-W*	*W-NW*	*NW-W*	*P$_M$*
B 4 ms^{-1}	0.004	0.007	0.008	0.001	0.008	0.006	0.005	0.012	0.05
D 1.5 ms^{-1}	0.073	0.122	0.134	0.020	0.134	0.110	0.093	**0.205**	0.89
D 4 ms^{-1}	0.005	0.008	0.009	0.001	0.009	0.007	0.006	0.014	0.06
P$_\varphi$	0.082	0.14	0.15	0.02	0.15	0.12	0.10	0.23	

The selected grid cell size is 10x10 m², as it was deemed the best choice for LNG bunkering related accident effect distances, after trial and error.

3.1. System Parameters

Piraeus is the largest and busiest port of Greece [3]. Every year, approximately 20 million passengers embark on a ship from Piraeus. As of today, the port can accommodate 3.5 million TEUs every year. Piraeus' annual passing vessel traffic is estimated to be over 24,000 vessels.

Meteorological Data concerning Piraeus, were sourced from publicly available information, provided by Piraeus' Meteorological Station [36]. A sample of the meteorological and location data that were utilised by the risk model, are shown in **Table 10**. The port of Piraeus does not present extreme meteorological conditions, which renders it an excellent candidate for LNG bunkering operations. Furthermore, the effect of obstructions on the atmospheric turbulence is assumed to be of minimal concern and it is therefore not considered.

The bunkering duration, rate, capacity, and frequency that were assumed, are shown in **Table 11**. The bunkering temperature and gauge pressure of LNG within the bunkering hose, is assumed to be 145 °C and 5 bar(g) respectively. As far as RoRo fuel capacity is concerned, the total capacities and average fuel consumptions of ferries that perform the Piraeus-Crete route were considered. Regarding the STS bunkering operation of a containership, a generic fuel capacity was assumed. Since

---

[4] Ship Striking

[5] f$_0$, is equal to 6.7·10^{-11}·T·t·N, where T is the total number of ships per year on the transport route or in the harbour, t is the average duration of loading/unloading per ship (in hours), and N is the number of transhipments per year.

LNG is about half as dense as conventional HFO, the quantity that must be bunkered (measured in metric tons at 25 °C) is about 1.8 times more.

Table 10. Location and Meteorological Assumptions.

Location	Air Temperature (°C)	Wind Speed (ms⁻¹)	Humidity (%)	Inversion (Y/N)
Port of Piraeus	20	3	69	No
Cloud Cover	Atmospheric Stability	Ground Roughness	Measurement Height	Wind Direction
3/10	D	150	3	NNW

Table 11. Various LNG Bunkering Assumed parameters.

Concept	Bunkering Source Capacity (m³)	Bunkering Rate (m³h⁻¹)	Receiving Vessel Type	Receiving Vessel Size (m³)	Bunkering Duration (h)	Bunkering Frequency (days/year)	Transhipments (per year)
TTS	50	600	RoRo	400	1	365	182
STS	600	600	RoRo	400	0.5	365	182
	2,500	1,000	Cont/ship	2,500	3	182	26

During an LNG bunkering operation, there can be an overwhelming number of places from where a potential leak may commence in case of an accident. It is therefore very important to explicitly outline the limits of the system whose safety is being assessed, to produce as accurate of a result as possible. Consequently, during the TTS operation, the area of interest is from the truck's LNG tank, up to the final Emergency Shutdown (ESD) valve before the vessel. Similarly, during STS bunkering, it is from the supplier's LNG tank, up to the receiving vessel's final ESD valve. Every other equipment that has the potential to fail, and is outside the limits stated above, is not taken into consideration. The cumulative time to detect and completely isolate a potential release, depending on the type of LOC, is shown in **Table 12**. It is noted that the smaller the accidental release, the greater the time it takes to be detected, especially when it comes to manifold leaks.

Table 12. Representative LOCs Shutdown time.

Scenario	Time to Shutdown (min)
Hose Leak	2
Hose Rupture	1
Manifold Leak	4
Manifold Rupture	1
Tank Rupture from S.S.[6]	1
Hose Rupture from S.S.	1

3.2. Risk Assessment

The result of the risk analysis procedure is the IR calculation which then must be compared with

---

[6] Ship Striking

an established set of IR criteria. Since the failure frequencies were sourced from the COVO 81 study, the IR criteria utilised are the ones adopted by the Dutch government [22]:

- Maximum tolerable risk for workers: **10^{-5} per year**
- Maximum tolerable risk for members of the public: **10^{-6} per year**
- Broadly acceptable (or negligible): **10^{-8} per year**

The above criteria represent safety distances for the installation of interest. For instance, when an LNG operation is under way, members of the public are not allowed in an area of the installation where IR levels are higher than 10^{-6} per year, which creates a minimum safety distance for members of the public.

In Figure 7 and Figure 8, the exported IR contours are presented for TTS and STS operations respectively. The safety distances that correspond to these contours are catalogued in Table 13. It is noted that in STS bunkering of a containership, larger IR contours are entailed, because substantially greater fuel quantities are involved. Moreover, for risk drivers to be identified, risk contribution is catalogued according to vessel type and loss of containment scenario. A risk driver constitutes an element of a system that has a high impact on risk and thus by improving its safety, IR is immensely reduced. The results, depending on the type of receiving vessel, are shown in Table 14 and Table 15. It is noted that the individual risk of bunkering a containership with LNG, is more than double compared to that of a Ro-Ro vessel. Furthermore, the risk drivers sorted by the LOC scenario, are shown in Table 16 and Table 17. Hose leaks and ruptures are major risk drivers when it comes to LNG bunkering.

Table 13. Individual Risk contour approximate region sizes.

Bunkering Concept	10-5 (m)	10-6 (m)	10-7 (m)	10-8 (m)
TTS	8	54	102	118
STS	21	79	322	510

Table 14. Risk contribution by client vessel, 20m away from source.

Receiving Vessel Type	Truck to Ship (TTS)		Ship to Ship (STS)	
	IR	*Risk Contribution*	*IR*	*Risk Contribution*
	(y^{-1})	*(%)*	*(y^{-1})*	*(%)*
RoRo	$3.1 \cdot 10^{-6}$	100	$6.2 \cdot 10^{-6}$	32.3
Containership	-	0	$1.3 \cdot 10^{-5}$	67.7
Total	$3.1 \cdot 10^{-6}$	100	$1.9 \cdot 10^{-5}$	100

Table 15. Risk contribution by client vessel, 100m away from source.

Receiving Vessel Type	Truck to Ship (TTS)		Ship to Ship (STS)	
	IR	*Risk Contribution*	*IR*	*Risk Contribution*
	(y^{-1})	*(%)*	*(y^{-1})*	*(%)*
RoRo	$2.9 \cdot 10^{-7}$	100	$7.1 \cdot 10^{-7}$	47.2
Containership	-	0	$7.4 \cdot 10^{-7}$	52.8
Total	$2.9 \cdot 10^{-7}$	100	$1.4 \cdot 10^{-6}$	100

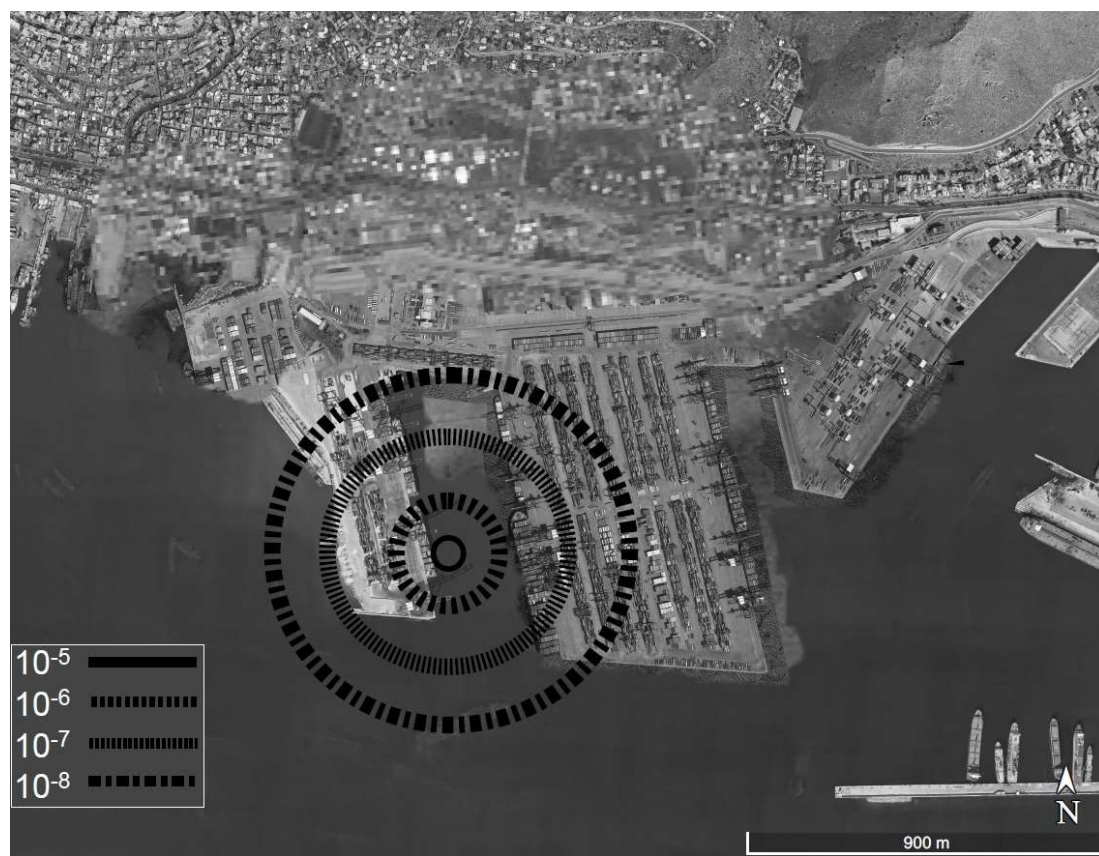**Figure 7.** TTS Individual Risk Contours.

Figure 8. STS Individual Risk Contours.

Table 16. Risk contribution by LOC, 20m away from source.

Receiving Vessel Type	Truck to Ship (TTS)		Ship to Ship (STS)	
	IR	Risk Contribution	IR	Risk Contribution
	(y^{-1})	(%)	(y^{-1})	(%)
Hose Leak	$2.9 \cdot 10^{-7}$	2.9	$8.7 \cdot 10^{-6}$	44.47
Hose Rupture	$8.6 \cdot 10^{-6}$	85.23	$1.0 \cdot 10^{-5}$	51.64
Manifold Leak	$2 \cdot 10^{-8}$	0.2	$1.0 \cdot 10^{-7}$	0.52
Manifold Rupture	$1.2 \cdot 10^{-6}$	11.67	$6.5 \cdot 10^{-7}$	3.3
Tank Rupture from S.S.[7]	-	-	$1.5 \cdot 10^{-8}$	0.07
Hose Rupture from S.S.	-	-	-	-
Total	$1.0 \cdot 10^{-5}$	100	$7.8 \cdot 10^{-6}$	100

Table 17. Risk contribution by LOC, 100m away from source.

Receiving Vessel Type	Truck to Ship (TTS)		Ship to Ship (STS)	
	IR	Risk Contribution	IR	Risk Contribution
	(y^{-1})	(%)	(y^{-1})	(%)
Hose Leak	-	-	$1.6 \cdot 10^{-7}$	9.08
Hose Rupture	$1.3 \cdot 10^{-6}$	87.95	$1.5 \cdot 10^{-6}$	84.4
Manifold Leak	-	-	-	-
Manifold Rupture	$1.8 \cdot 10^{-7}$	12.05	$1.1 \cdot 10^{-7}$	6.52
Tank Rupture from S.S.[8]	-	-	-	-
Hose Rupture from S.S.	-	-	-	-
Total	$1.5 \cdot 10^{-6}$	100	$1.7 \cdot 10^{-6}$	100

It is noted that the above QRA methodology is modular. Therefore, even though it constitutes an application of the proposed QRA model in the case study of Piraeus, it could also be applied on a wide variety of establishments throughout the world.

4. Discussion

A QRA is a process that may be ambiguous due to the vast number of parameters that are specific to the site whose safety is being assessed. Even though the proposed QRA methodology is modular, the results of this case study, are site-specific to the STS and TTS operations, that will commence at the Port of Piraeus in the future.

The equipment failure frequencies used, are based on the COVO 81 study [26]. The LNG bunkering industry hasn't yet substantially grown and as a result, there is a lack of failure frequencies. Until then, the failure frequencies that are utilised will predominantly be pertinent to generic hydrocarbon releases, where higher failure rates are entailed compared to LNG specifically.

Depending on the bunkering site, the equipment and the scenario, variables such as the port's obstructions, vessel's capacity, bunkering flow rate, bunkering duration, bunkering frequency and transhipments, may vary. The absolute pressure inside the bunkering hoses might be different than

---

[7] Ship Striking

[8] Ship Striking

the one assumed as well, depending on the application and the equipment used.

The quantification of thermal radiation zones and cloud dispersion characteristics were attained with the employment of ALOHA (Areal Locations of Hazardous Atmospheres) [33]. Input variables such as the properties of the released chemical, air temperature, ground roughness, atmospheric stability, humidity, cloud cover, wind speed, wind direction, altitude, details about the spill scenario and a wide variety of other parameters were used. Also, since a cold natural gas cloud disperses downwind as a dense gas, a Heavy Gas Dispersion model was utilised.

4.1. Comparison With Other Studies

After probabilistic safety zones have been established, having them compared with results from other research, constitutes a common practice. The studies that were utilised, stem from DNV [1] and Fluxys LNG [10]. DNV's study concerned the port of Los Angeles, whereas Fluxys' considered the Flemish ports. Their proposed safety zones are presented in **Table *18***. The suggested safety distances that emanated from the Piraeus' case study, are predominantly of similar magnitude to the corresponding results of DNV and Fluxys. In particular, the application of the proposed risk model, produces safety zones with a level of IR$\leq 10^{-5}$, that are smaller. On the contrary, for levels of IR $\in$ [10^{-7},10^{-6}], the proposed safety distances are larger than the corresponding ones from DNV and Fluxys. However, it is noted that in some instances (e.g., $STS_{IR}=10^{-7}$), there is significant deviation, which is something to be expected, since the QRAs concern different establishments, with dissimilar system parameters (e.g., meteorological conditions, incoming traffic, size of accommodated vessels, etc.).

Table 18. Comparison of IR Contours.

Risk Acceptance Criteria	Piraeus QRA (m)		DNV (m)		Fluxys (m)	
	TTS	*STS*	*TTS*	*STS*	*TTS*	*STS*
10^{-5}	8	21	12	15	24	36
10^{-6}	54	79	46	60	38	72
10^{-7}	102	322	73	275	54	198

4.2. Formal Safety Assessment

A Formal Safety Assessment (FSA) [37] is a structured and systematic methodology, aimed at enhancing maritime safety, including protection of life, health, the marine environment and property, by using risk analysis and cost benefit assessment. It consists of a Hazard Identification (HazID), a risk assessment, risk control options, a cost benefit assessment, and recommendations for decision-making.

An FSA is a useful tool for the rule-making process in the maritime industry [38]. However, since in this study, the safety of an entire fleet of vessels is not assessed, an FSA would be outside of its scope. A QRA is a source analysis, that is more than capable of drawing conclusions that will assist the work of the regulatory bodies and enhance the safety of the LNG bunkering industry, as it continues to increase in size. As a result, a QRA on evaluating the safety of LNG bunkering, suffices.

4.3. Regulatory Framework

The three most pertinent stakeholders concerning the implementation of LNG bunkering rules and regulations, are classification societies, flag administrations and port authorities.

The IMO regulations that are applicable to LNG bunkering are [39]: the SOLAS (Safety Of Life At Sea) convention including fuel requirements, the STCW (Standards of Training, Certification and Watchkeeping) for Seafarers convention including special crew training requirements, the International Code for Construction and Equipment of Ships Carrying Liquefied Gases in Bulk (IGC Code) including requirements for the construction and operation of LNG tankers, the MSC.285(86) (Maritime Safety Committee): Interim Guidelines on Safety for Natural Gas-Fuelled Engine Installations in Ships and the International Code of Safety for Ships using Gases or other low Flashpoint Fuels (IGF Code) including requirements for the construction and operation of gas-fuelled ships.

The reports issued by ISO regarding LNG bunkering are Guidelines for systems and installations for supply of LNG as fuel to ships (ISO 118683, 2013), Guidance on performing risk assessment in the design of onshore LNG installations including the ship/shore interface (ISO 116901, 2013) and Specifications for bunkering of liquefied natural gas fuelled vessels (ISO 20519, 2017).

Norway has been conducting LNG bunkering operations for almost a decade now [40]. As the LNG infrastructure around Europe expands, so will the regulatory framework. The European Maritime Safety Agency (EMSA) issued an LNG bunkering study, titled ``Guidance on LNG Bunkering to Port Authorities and Administrations'', where all the regional, national and international rules and regulations that apply to LNG bunkering, are catalogued [39]. In addition, regulatory gaps are identified to be addressed by regulators.

Greece issued Presidential Decree 64/2019, in the Official Government's Gazette Issue No. 103/A/20-6-2019, where guidelines applying to the safety of using LNG as a maritime fuel are included. Among these guidelines, are parameters such as safety equipment, fire safety, bunkering procedures' outline and duration, SIMOPS, training needs and many more.

All the rules and regulations can be augmented by the findings and recommendations of a QRA. Therefore, the results of this case study can be employed as guidelines, to enrich the regulatory framework of LNG bunkering in Greece.

5. Conclusions

According to the outcome of the case study, the risk entailed in STS operations is substantially higher than TTS, which is justified by the fact that TTS is a restrictive procedure, not only in its bunkering capacity and rate, but in its applicability as well. On the contrary, during STS, flexibility is provided, as both ferries and containerships can be accommodated. The drawback of servicing large ships such as containerships, however, is the increased risk that is associated with the procedure, since if there is an accidental event, the repercussions will be far more severe.

IR during STS becomes negligible ($\leq 10^{-8}$) at 510 m (**Table 13**). However, the bunkering operation can be performed in the open sea, away from the installations of a port, which renders the calculated safety distances manageable. Furthermore, the people on board a containership, are trained seamen that accept the higher risk their job entails, and in the instance of an accident they are fully aware of their surroundings as well as the first actions that must be performed. TTS is a valid option for low capital investment and small vessels' refuelling. Nevertheless, STS is more practical and flexible.

The benefits of a probabilistic safety study are reflected on the results of this QRA (**Table 13** to **Table 17**). For instance, an LNG, double wall, type C tank rupture, is a predicament which leads to

catastrophic consequences and has the potential to spread heat and fragments through thousands of meters. However, since its failure frequency is extremely low, it is not a significant risk driver. Hose ruptures however, are. Loading hose failure may occur either due to an equipment failure, a ship striking, or even human error. Hence their higher frequency rates, renders them the dominant risk driver.

The expansion of the global LNG bunkering infrastructure presents not only economical but social benefits as well. Due to the reduced harmful emissions, the area around a busy port such as Piraeus, will become more inhabitant friendly. It is noted, that due to the modular nature of the proposed risk model, it can be further utilised in a wide variety of areas, ports, and locations where LNG bunkering may take place.

5.1. Recommendations

The key outcome of this paper is the accentuation of the benefits entailed in risk-based design. The identification of risk drivers in a complex system is a cumbersome task that can be assisted by a QRA. Therefore, it is recommended that during the development of the regulatory framework, infrastructure and common practices in the LNG bunkering industry, risk-based criteria are to be met in every step of the process. In addition, whenever possible, a QRA is to be preferred over a QualRA, since more credible results are produced. It is noted, that the proposed QRA methodology can also be employed for the estimation of Societal Risk and external costs, which will be demonstrated in the authors' future work.

Hose ruptures are the most significant risk driver. They are relatively frequent and can lead to catastrophic outcomes. The accidents associated with hose ruptures are caused by either human error or equipment failure. It is therefore recommended that during LNG bunkering operations, the industry's standard practices are followed to the letter, to mitigate human factors as much as possible.

Supplementary Materials: The following are available online at www.mdpi.com/xxx/s1, Figure S1: title, Table S1: title, Video S1: title.

Conflicts of Interest: The authors declare no conflict of interest.

References

[1] DNV GL, "Liquefied Natural Gas (LNG) Bunkering Study Maritime Administration," DNV GL, PP087423-4, Rev 3, Sep. 2014. [Online]. Available: https://www.academia.edu/27700880/Liquefied_Natural_Gas_LNG_Bunkering_Study_Maritime_Administration.

[2] Rall David P., "Review of the Health Effects of Sulfur Oxides," *Environmental Health Perspectives*, vol. 8, pp. 97–121, Aug. 1974. DOI: https://doi.org/10.1289/ehp.74897.

[3] S. D. Chatzinikolaou, S. D. Oikonomou, and N. P. Ventikos, "Health externalities of ship air pollution at port – Piraeus port case study," *Transportation Research Part D: Transport and Environment*, vol. 40, pp. 155–165, Oct. 2015. DOI: https://doi.org/10.1016/j.trd.2015.08.010.

[4] IMO, Marpol: articles, protocols, annexes, unified interpretations of the International Convention for the Prevention of Pollution from Ships, 1973, as modified by the Protocol of 1978 relating thereto. 2017. [Online]. Available: http://www.imo.org/en/About/Conventions/ListOfConventions/Pages/International-Convention-for-the-Prevention-of-Pollution-from-Ships-(MARPOL).aspx.

[5] IMO, "Studies of the feasibility and use of LNG as fuel for shipping," p. 290, 2016.

[6]   O. Aneziris, I. Koromila, and Z. Nivolianitou, "A systematic literature review on LNG safety at ports," *Safety Science*, vol. 124, p. 104595, Apr. 2020. DOI: https://doi.org/10.1016/j.ssci.2019.104595.

[7]   ABS, "Bunkering of Liquefied Natural Gas-fueled Marine Vessels in North America," ABS, 2015. [Online]. Available: https://ww2.eagle.org/content/dam/eagle/publications/reference-report/LNG-Bunkering-NAmerica-2015.pdf.

[8]   ISO, *Guidelines for systems and installations for supply of LNG as fuel to ships ISO/TS 18683:2015*. 2015. Accessed: Sep. 02, 2020. [Online]. Available: https://www.iso.org/standard/63190.html.

[9]   DNV GL, "Development and operation of liquefied natural gas bunkering facilities," DNV GL, Oct. 2015. [Online]. Available: https://www.dnvgl.com/oilgas/download/dnvgl-rp-g105-development-and-operation-of-liquefied-natural-gas-bunkering-facilities.html.

[10]   Fluxys LNG, "Supplying Flemish ports with LNG as a marine fuel," Fluxys LNG, 2012. [Online]. Available: https://www.researchgate.net/publication/321825365_Risk_assessment_Study_-_Supplying_Flemish_ports_with_LNG_as_a_marine_fuel_-_Final_Report.

[11]   J. L. Woodward and R. Pitbaldo, *LNG Risk Based Safety: Modeling and Consequence Analysis*. Wiley, 2010. [Online]. Available: https://www.wiley.com/en-us/LNG+Risk+Based+Safety%3A+Modeling+and+Consequence+Analysis-p-9780470317648.

[12]   R. G. Scurlock, *Stratification, Rollover and Handling of LNG, LPG and Other Cryogenic Liquid Mixtures*, 1st ed. 2016 edition. Cham: Springer, 2015. DOI: https://doi.org/10.1007/978-3-319-20696-7.

[13]   S. Mokhatab, J. Y. Mak, J. V. Valappil, and D. A. Wood, *Handbook of Liquefied Natural Gas*, 1st edition. Amsterdam Boston Heidelberg: Gulf Professional Publishing, 2016. ISBN-13: 978-0128099964.

[14]   S. Huang, C.-H. Chiu, and D. Elliot, *LNG: Basics of Liquefied Gas*, 1st edition. Austin: The University of Texas at Austin - Petroleum Extension Service, 2007. ISBN-13: 978-0886982171.

[15]   A. Bulte, *Fundamentals of LNG Process Engineering: A guide in LNG Fundamentals*. Place of publication not identified: Independently published, 2017. ISBN: 9781520993232.

[16]   IMO, *IGF code: international code of safety for ships using gases or low flashpoint fuels*. 2016. [Online]. Available: http://www.imo.org/en/OurWork/Safety/SafetyTopics/Pages/IGF-Code.aspx.

[17]   H. J. Pasman, Risk Analysis and Control for Industrial Processes - Gas, Oil and Chemicals: A System Perspective for Assessing and Avoiding Low-Probability, High-Consequence Events, 1st edition. Amsterdam: Butterworth-Heinemann, 2015. ISBN: 9780128000571.

[18]   L. Ostrom and C. Wilhelmsen, "Probabilistic Risk Assessment," in *Risk Assessment*, John Wiley & Sons, Ltd, 2019, pp. 251–260. DOI: https://doi.org/10.1002/9781119483342.ch17.

[19]   R. Bubbico, "Efficient Applications of Risk Analysis in the Chemical Industry and Emergency Response," *Journal of Risk Analysis and Crisis Response*, vol. 1, no. 2, pp. 92–101, Art. no. 2, 2011, Accessed: Nov. 26, 2021. [Online]. Available: https://jracr.com/index.php/jracr/article/view/49. DOI: https://doi.org/10.2991/ijcis.2011.1.2.1.

[20]   M. Elmontsri, "Review of the strengths and weaknesses of risk matrices," *Journal of Risk Analysis and Crisis Response*, vol. 4, no. 1, pp. 49–57, Art. no. 1, 2014, Accessed: Nov. 25, 2021. [Online]. Available: https://jracr.com/index.php/jracr/article/view/99. DOI: https://doi.org/10.2991/jrarc.2014.4.1.6.

[21]   CCPS, *Guidelines for Risk Based Process Safety*, 1st edition. Hoboken, N.J: Wiley-AIChE, 2007.

[22]   RIVM, CPR, and VROM, *Guidelines for quantitative risk assessment*, vol. 3, 4 vols. PublicatiereeksU Gevaarlijke Stoffen, 2005. [Online]. Available: https://publicatiereeksgevaarlijkestoffen.nl/publicaties/PGS3.html.

[23]   R. Turney, *Risk Assessment in the Process Industries - IChemE*, 2r.e. edition. Rugby: Institute of Chemical Engineers, IChemE, 1996. ISBN-13: 978-0852953235.

[24]   H. K. Fauske and M. Epstein, "Source term considerations in connection with chemical accidents and vapour cloud modelling," *Journal of Loss Prevention in the Process Industries*, vol. 1, no. 2, pp. 75–83, Apr. 1988. DOI: https://doi.org/10.1016/0950-4230(88)80016-0.

[25]   J. A. Havens and T. O. Spicer, "Development of an atmospheric dispersion model for heavier-than-air gas mixtures. Volume 3. DEGADIS user's manual. Final report, September 1980-May 1985," Arkansas Univ., Fayetteville (USA). Dept. of Chemical Engineering, AD-A-171524/2/XAB, May 1985. Accessed: Feb. 24, 2021. [Online]. Available: https://www.osti.gov/biblio/6991746-development-atmospheric-dispersion-model-heavier-than-air-gas-mixtures-volume-degadis-user-manual-final-report-september-may.

[26] RIVM, CPR, and VROM, *Methods for the determination of possible damage*, vol. 1, 4 vols. PublicatiereeksU Gevaarlijke Stoffen, 2005. [Online]. Available: https://publicatiereeksgevaarlijkestoffen.nl/publicaties/PGS1.html.

[27] F. Pasquill, "The Estimation of The Dispersion of Windborne Material," *Meteorological Magazine*, vol. 90, no. 1063, 1961, Accessed: Dec. 14, 2020. [Online]. Available: https://ci.nii.ac.jp/naid/10010457582/en/.

[28] F. a. J. Gifford, "Use of routine meteorological observations for estimating atmospheric dispersion," *undefined*, 1961. /paper/Use-of-routine-meteorological-observations-for-Gifford/19110d239630e9b0f64b9df935e0f88d2c4d8e9d (accessed Dec. 14, 2020).

[29] J. Cook, Z. Bahrami, and R. J. Whitehouse, "A comprehensive program for calculation of flame radiation levels," *Journal of Loss Prevention in the Process Industries*, vol. 3, no. 1, pp. 150–155, Jan. 1990. DOI: https://doi.org/10.1016/0950-4230(90)85039-C.

[30] J. Moorhouse and M. J. Pritchard, "Thermal radiation hazards from large pool fires and fireballs: a literature review," Jan. 1982, Accessed: Feb. 24, 2021. [Online]. Available: https://www.osti.gov/etdeweb/biblio/6552741.

[31] F. Kadri, E. Chatelet and P. Lallement, "The Assessment of Risk Caused by Fire and Explosion in Chemical Process Industry: A Domino Effect-Based Study," *Journal of Risk Analysis and Crisis Response*, vol. 3, no. 2, Art. no. 2, 2013, Accessed: Nov. 26, 2021. [Online]. Available: https://jracr.com/index.php/jracr/article/view/80. DOI: https://doi.org/10.2991/jrarc.2013.3.2.1.

[32] ISO, Ships and marine technology. specification for bunkering of liquefied ... [bs en iso 20519: 2017. Place of publication not identified: BSI, 2017.

[33] R. Jones, W. Lehr, D. Simecek-Beatty, and M. Reynolds, "ALOHA (Areal Locations of Hazardous Atmospheres): Technical Documentation," p. 96, 2016.

[34] CCPS, Guidelines for Evaluating the Characteristics of Vapor Cloud Explosions, Flash Fires, and BLEVEs, 1st edition. New York, NY: Wiley-AIChE, 1994. ISBN:9780816904747.

[35] N. Eisenberg, C. Lynch, and R. Breeding, "Vulnerability Model. A Simulation System for Assessing Damage Resulting from Marine Spills," p. 355, Jun. 1975.

[36] Meteo.gr, "Weather Data," *Meteo*, 2019. http://meteosearch.meteo.gr/stationInfo.asp (accessed Sep. 02, 2020).

[37] IMO, "Revised guidelines for Formal Safety Assessment (FSA) for use in the IMO rule-making process." 2018. [Online]. Available: https://www.imo.org/en/OurWork/Safety/Pages/FormalSafetyAssessment.aspx.

[38] J. Wang *et al.*, "Use of Advances in Technology for Maritime Risk Assessment," *Risk Analysis*, vol. 24, no. 4, pp. 1041–1063, 2004. DOI: https://doi.org/10.1111/j.0272-4332.2004.00506.x.

[39] EMSA, "Guidance on LNG bunkering to port authorities and administrations," 2018. [Online]. Available: https://safety4sea.com/wp-content/uploads/2018/02/EMSA-Guidance-on-LNG-Bunkering-to-Port-Authorities-and-Administrations-2018_02.pdf.

[40] S. Laribi and E. Guy, "Promoting LNG as A Marine Fuel in Norway: Reflections on the Role of Global Regulations on Local Transition Niches," *Sustainability*, vol. 12, no. 22, p. 9476, Nov. 2020. DOI: https://doi.org/10.3390/su12229476.